Eur. Phys. J. Appl. Phys. **51**, 20901 (2010)
DOI: 10.1051/epjap/2010087

THE EUROPEAN PHYSICAL JOURNAL APPLIED PHYSICS

Regular Article

Comparison of Pd/D co-deposition and DT neutron generated triple tracks observed in CR-39 detectors

P.A. Mosier-Boss[1,a], J.Y. Dea[1], L.P.G. Forsley[2], M.S. Morey[3], J.R. Tinsley[3], J.P. Hurley[3], and F.E. Gordon[4]

[1] SPAWAR Systems Center Pacific, Code 71730, San Diego, CA 92152, USA
[2] JWK International Corp., Annandale, VA 22003, USA
[3] National Security Technologies, LLC, Special Technologies Laboratory, Santa Barbara, CA 93111, USA
[4] SPAWAR Systems Center Pacific, Retired, San Diego, CA 92122, USA

Received: 28 February 2010 / Received in final form: 5 May 2010 / Accepted: 20 May 2010
Published online: 7 July 2010 –

Abstract. Solid state nuclear track detectors (SSNTDs), such as CR-39, have been used to detect energetic charged particles and neutrons. Of the neutron and charged particle interactions that can occur in CR-39, the one that is the most easily identifiable is the carbon breakup reaction. The observation of a triple track, which appears as three alpha particle tracks breaking away from a center point, is diagnostic of the $^{12}C(n, n')3\alpha$ carbon breakup reaction. Such triple tracks have been observed in CR-39 detectors that have been used in Pd/D co-deposition experiments. In this communication, triple tracks in CR-39 detectors observed in Pd/D co-deposition experiments are compared with those generated upon exposure to a DT neutron source. It was found that both sets of tracks were indistinguishable. Both symmetric and asymmetric tracks were observed. Using linear energy transfer (LET) curves and track modeling, the energy of the neutron that created the triple track can be estimated.

1 Introduction

In 1978, Cartwright et al. [1] were the first to demonstrate that Columbia Resin 39 (CR-39), an optically clear, amorphous, thermoset plastic, could be used to detect nuclear particles. When an energetic, charged particle traverses through a solid state nuclear track detector (SSNTD) such as CR-39, it creates along its path an ionization trail that is more sensitive to chemical etching than the bulk material [1,2]. After treatment with a chemical etchant, tracks due to the energetic particles remain in the form of holes or pits which can be examined with the aid of an optical microscope. The size, depth of penetration, and shape of the track provides information about the mass, charge, energy, and direction of motion of the particle that created the track [3]. Besides detection of charged particles such as protons and alphas, CR-39 can also be used to detect neutrons [4].

Since its introduction as a detector for nuclear particles, CR-39 has found extensive use as a charged-particle spectrometer to study inertial-confinement-fusion (ICF) plasmas [4]. This is not surprising given the ability of CR-39 to detect both energetic charged particles and neutrons, which are products of the fusion reactions that occur in the plasma created upon laser-compression of the fuel capsule. Other advantages of CR-39 for use in the ICF field are its integrating capability, existence of a threshold for registration, ruggedness, and a degree of charge and energy discrimination [5]. SSNTDs can be used to record events cumulatively over long periods of time. This is particularly important for events that occur either sporadically or in bursts. The detectors are insensitive to electromagnetic noise and are resistant to mechanical damage. CR-39 detectors are relatively insensitive to gamma or X-ray emissions. Dielectric materials, such as CR-39, can register particles only if their charge and linear energy transfer (LET) value are above a minimum threshold that is dependent upon the composition and structure of the detector. A great deal of effort has been spent by a number of researchers to calibrate the SSNTDs using particle generators for speciation and energy determination [6]. While the size and shape of the track depends upon the energy and charge of the particle that created it, the ability of the detectors to discriminate particles is still poor and is dependent upon etching conditions and methodology. This is compounded by variability between the detectors caused by manufacturing procedures, the age of the detectors, as well as the temperature and storage history of the detectors.

The same advantages that make CR-39 useful in the ICF community also make it attractive for use in detecting particles in the Pd/D system. In addition, the

[a] e-mail: pam.boss@navy.mil

inherent spatial resolution of the CR-39 detectors is advantageous in that it can potentially be used to spatially correlate active Pd sites with energetic particle production. CR-39 detectors have been used to detect energetic particles in both Pd/D gas-loading [7] and electrolytic-loading experiments [8–12]. More recently, detection of particles using CR-39 detectors was demonstrated for the Pd/D co-deposition process, in which palladium is electroplated onto a non-hydriding metal surface [13]. A series of control experiments showed that the optical properties of the observed Pd/D co-deposition tracks were consistent with those observed for nuclear particle generated tracks, that the tracks were not due to radioactive contamination of the cell components, nor were the tracks due to either chemical or mechanical damage [14]. Additional experiments placing Mylar spacers between the CR-39 detectors and the cathode indicated that the majority of the particles, after traversing through a thin water film, had energies on the order of 1 MeV by the time they reached the detector [15]. It was also reported that tracks had been observed on the backside of the CR-39 detectors used in Pd/D co-deposition experiments and that these tracks were consistent with those due to neutron recoils [16]. Sequential etching of the detectors showed the presence of tracks deeper inside the detector that are attributed to neutron recoils [16,17]. In addition to solitary tracks, triple tracks have been observed in CR-39 detectors used in Pd/D co-deposition experiments [17]. Triple tracks, in which three particles are breaking away from a center point, are indicative of a reaction that produces three particles of equal mass and energy conservation. In this communication, Pd/D co-deposition generated triple tracks are compared with DT neutron generated tracks. The origins of these triple tracks are discussed.

2 Experimental

Palladium was plated out from a 0.03 M $PdCl_2$ and 0.3 M LiCl in D_2O onto either a non-hydriding metal cathode or a Pd wire in either the presence or absence of an external magnetic field. Details on cell design and operation have been described elsewhere [14–16]. Unless otherwise indicated, experiments typically ran over a two week period. The solid state nuclear track detector (SSNTD), CR-39, was used in one of three experimental configurations. Some experiments were conducted with the cathode in direct contact with the CR-39 detector. Other experiments were conducted with a 60 μm thick polyethylene film between the detector and the cathode. In this experimental configuration, the polyethylene film acts as a neutron radiator, charged particle filter, and mechanical/chemical barrier. In the third experimental configuration, the CR-39 detector was placed outside the cell but adjacent to a 0.25 mm diameter Pd wire with a thin electroplated coating of Pd. A 75 μm Mylar film separated the CR-39 detector and the cathode. Experimental conditions are noted in the figure captions. Upon completion of the experiment, the cell was disassembled and the CR-39 detector was etched in 6.5 M NaOH for six hours at 62 °C. Afterwards, the CR-39 detector was subjected to microscopic analysis using an Eclipse E600 epifluorescent microscope (Nikon) and images were taken using a CoolSnap HQ CCD camera (Photometrics).

CR-39 detectors were exposed to DT neutrons generated by a Thermo Fisher model A290 neutron generator. The detectors were exposed to a neutron flux of 10^7 neutrons s^{-1} for 4.5 h. Afterwards the detectors were etched and subjected to microscopic analysis as described above.

3 Results and discussion

3.1 The use of CR-39 to detect neutrons

Because they have no charge, there is no direct method to detect neutrons. Instead indirect methods are used in which the neutrons are allowed to interact with other atomic nuclei and the response of that interaction is measured [18]. These methods fall in one of two categories – neutron capture or elastic scattering. In the neutron capture method, the target nucleus captures the neutron to create an unstable nucleus that spontaneously loses energy by emitting ionizing particles or gamma/X-rays. These radioactive decay products are then detected. However, since the cross section for neutron capture is lower at high neutron energies, this method requires the use of moderators to slow the neutrons down so that capture can occur. Consequently, the energy of the neutron can not be determined by this method. In the elastic scattering method, the neutron scatters off nuclei causing the struck nucleus to recoil. The recoiling nucleus can ionize and excite additional atoms through collisions producing charge and/or scintillation light which are then detected. These types of detectors do not require a moderator so that the energy of the neutrons can be determined. However these detectors also respond to gamma/X-rays and require a discriminator. About 15 years ago, the use of Au foil activation to detect neutrons in the Pd/D co-deposition experiments was explored. This is an example of a neutron capture method of detection. However, no signals above background were detected and it was concluded that either the method of detecting the gamma emissions (liquid scintillation) was not sensitive enough, the neutron energies were not compatible with detection using Au foils, or the rate of neutron production was too low to detect by this method.

There are other problems with electronic neutron detectors. Electronic neutron detectors can be subject to low level electronic noise picked up from the local environment. For example, Jones et al. [19] retracted claims of neutron emissions from Pd/LiOD electrolytic cells when it was found that the large bursts they were seeing with their ^{3}He detectors were actually the result of high voltage breakdown in the electronics. Besides electronic noise, these detectors are temperature sensitive. Typically long acquisition times are used to improve the signal to noise ratio. If the rate of neutron production is sporadic and/or at a low level, the resultant signal can be averaged away.

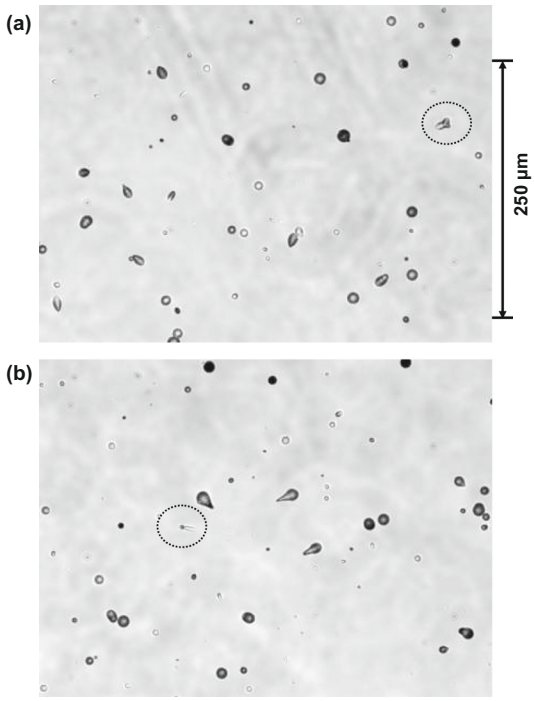

Fig. 1. Two photomicrographs of DT neutron generated tracks in CR-39 at 200× magnification. Both images were taken from the same CR-39 detector. (a) A triple track is circled. This triple track formed near the surface of the detector. (b) The triple track circled is smaller than the one shown in (a). This track was generated deeper inside the plastic.

Another problem is if multiple neutrons hit the detector at the same time, the discriminator will reject the signal. In contrast CR-39 detectors do not suffer from these issues. In addition, the integrating capability of CR-39 makes it advantageous for detecting neutrons that are generated at either a low rate or in bursts. As discussed vide supra, CR-39 has been used to detect neutrons and these detectors are widely used in neutron dosimeters and in inertial confinement fusion (ICF) to characterize the imploded core density [4,5].

In order to detect neutrons with CR-39, the neutron must either scatter or undergo a nuclear reaction with the proton, carbon, or oxygen atoms comprising the detector to form a moving charged particle. It is the track of this neutron-generated charged particle that is revealed upon etching. Phillips et al. [20] have shown that the CR-39 track-size can be used to distinguish neutron energies between 0.144−1.2 MeV and 8.0−19.0 MeV, but that this method is ambiguous from 1.2−8.0 MeV. Lipson et al. [21] resolved the interval between 1 and 4 MeV by using calibrated proton sources normal to the surface, since energetic proton and energetic neutron-induced proton recoils will leave identical tracks subject to the Linear Energy Transfer function of the solid state nuclear track detector. Figure 1 shows photomicrographs of DT neutron generated tracks in a CR-39 detector. Based upon the results of Phillips et al. [20], the small tracks are identified as proton recoils while the larger circular and elliptical tracks are attributed to carbon/oxygen recoils. The proton recoils are observed at neutron energies as low as 0.144 MeV. The carbon/oxygen recoils have an energy threshold of 1.2 MeV. In both photomicrographs, a triple track is observed. These triple tracks are diagnostic of the ^{12}C(n, n′)3α carbon breakup reaction in the detector with an energy threshold of ≥9.6 MeV [22–25]. Neutron interactions with the detector can occur anywhere inside the detector. It can be seen that the triple track in Figure 1b is significantly smaller than the one in Figure 1a. As both images in Figure 1 were taken from the same CR-39 detector, the difference in size indicates that the neutron interaction that caused the triple track in Figure 1b occurred deeper inside the plastic than the one that caused the triple track in Figure 1a.

3.2 Comparison of overlapping tracks and DT neutron generated tracks

By focusing inside the tracks it is possible to differentiate overlapping tracks from triple tracks resulting from the carbon break-up reaction. Figure 2a shows photomicrographs of "triple tracks" resulting from overlapping (i) ∼5 MeV and (ii) ∼1 MeV alpha tracks. The left hand images were obtained by focusing the microscope optics on the surface of the detector. The outlines of the overlapping tracks are clearly visible. The right hand images were obtained by overlaying two images taken at different focusing depths – the surface of the detector and the bottom of the pits. A distinct, separate, bright spot is observed in each of the overlapping tracks. The bright spot indicates the endpoint for the particle that entered the detector [3]. These separate bright spots inside the overlapping tracks show that the particles that created each track reached the detector at different times, i.e., the three lobes of the apparent "triple track" in Figures 2a(i) and 2a(ii) are not related to a single event. This contrasts with what is observed for DT neutron generated triple tracks shown in Figure 2b. In Figure 2b, the left hand image was obtained by focusing the microscope optics on the surface of the detector and the right hand image is an overlay of two images taken at different focusing depths (surface and bottom of the tracks). The surface image shows three overlapping tracks. By focusing the microscope optics inside the triple tracks (right hand images), it can be seen that the individual lobes making up the triple tracks are emanating from a center point. These features, which are characteristic of the carbon breakup reaction, make it easy to differentiate this reaction from neutron recoils, charged particle tracks and background events and show that CR-39 is ideally suited for detecting neutrons with energies ≥9.6 MeV.

How the DT generated triple tracks were created is described in Figures 2c and 2d. Figure 2c(i) is the overlay images of the DT neutron generated triple track shown in Figure 2b(i). Arrows indicate the direction the alphas moved after the carbon atom was shattered by the neutron. In Figure 2c(i), the circled area indicates where the three lobes of the triple track meet. The bright spots at the end of the lobes in Figure 2c(i) indicate the endpoints

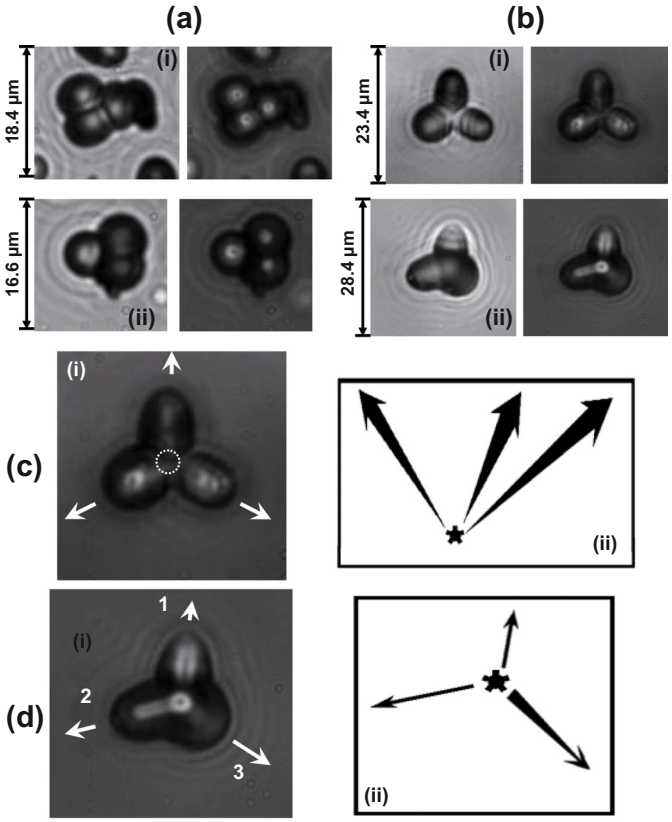

Fig. 2. (a) Overlapping tracks observed in CR-39 detectors exposed to (i) ∼5 MeV alphas from an ^{241}Am source (1000× magnification) and (ii) ∼1 MeV alphas created by placing 18 μm of Mylar between a uranium wire and the CR-39 detector (1000× magnification). (b) Triple tracks produced upon exposure to DT generated neutrons. In both (a) and (b), the left-hand image was obtained with the optics focused on the surface of the CR-39 detector while the right-hand image is an overlay of two photomicrographs taken at different focusing depths (surface of the detector and the bottom of the pits). (c) Left hand microphotograph is the overlay image of the DT neutron generated triple track shown in b(i). The arrows indicate the directions the alphas moved after the carbon atom shattered. The circled area indicates where the three lobes of the triple track meet. The right hand image is a schematic showing how the triple track was created when the carbon atom (star) shattered by the DT neutron (n). (d) Left hand microphotograph is the overlay image of the DT neutron generated triple track shown in b(ii). The arrows indicate the directions the alphas moved after the carbon atom shattered. The right hand image is a schematic showing how the triple track was created when the carbon atom (star) shattered.

for the alphas when they came to rest. Figure 2c(ii) shows a side view schematic of the carbon breakup reaction that created the triple track shown in Figure 2c(i). In Figure 2d(i), the bright circle indicates where the DT neutron collided with the carbon atom causing it to shatter into three alphas. Tracks 1 and 2 are near the surface of the detector while track 3 goes deeper inside the detector. Figure 2d(ii) describes the breakup reaction that resulted in the triple track shown in Figure 2d(i).

3.3 Comparison of Pd/D Co-deposition and DT generated triple tracks in CR-39 SSNTDs

Triple tracks in CR-39 detectors used in Pd/D co-deposition experiments were previously reported [17]. The Pd/D co-deposition experiments using CR-39 detectors typically last two weeks. Tracks, as well as triple tracks, have been observed when Pd/D co-deposition has been done on Ag, Au, and Pt wires in both the presence and absence of an external electric/magnetic field [14]. These tracks have been observed on the front and back surfaces of the detectors [16]. No tracks on CR-39 were observed for Pd/D co-deposition done on a Ni screen in the absence of an external electric/magnetic field [14]. However, in the presence of an external electric/magnetic field, tracks have been obtained in CR-39 when Pd/D co-deposition has been done on Ni screen. The role played by the cathode material (Ag/Au/Pt wire vs. Ni screen) and external fields on the formation of tracks is still not fully understood. The number of triple tracks observed in the CR-39 detectors used in Pd/D co-deposition experiments is low, at most 5 to 10 tracks/detector, including both the front and back surfaces. Such tracks have not been observed in background monitoring detectors or in detectors used in control experiments. These triple tracks were detected in areas where the track density was low enough to positively identify them from the background of single tracks. As discussed vide supra, by focusing inside the tracks, overlapping tracks can be easily differentiated from triple tracks resulting from the carbon break-up reaction.

To verify that the triple tracks observed in the Pd/D co-deposition experiments are consistent with those observed as the result of the carbon break-up reaction, CR-39 detectors were exposed to an accelerator-driven DT fusion neutron source and etched. Figures 3 and 4 show side-by side comparisons of triple tracks in CR-39 detectors produced as a result of Pd/D co-deposition experiments (Figs. 3a and 4a) and those created upon exposure to a DT neutron source (Figs. 3b and 4b). For the respective triple tracks shown in Figures 3a, 3b and 4a, 4b, the left-hand images are obtained by focusing the microscope optics on the surface of the detector. The right-hand images in Figures 3a, 3b and 4a, 4b are an overlay of two microphotographs taken at two different focusing depths – the surface of the detector and the bottom of the tracks. The Pd/D co-deposition experimental details are described in the figure captions. In general, three experimental configurations were employed. Some experiments were conducted with the cathode in direct contact with the CR-39 detector, Figures 3a(i) and 3a(ii). Other experiments were conducted with a 60 μm thick polyethylene film, acting as a neutron radiator, charged particle filter, and mechanical/chemical barrier, between the detector and the cathode, Figures 3a(iii), 3a(iv), 4a(i), and 4a(iii). In the third experimental configuration, the CR-39 detector was placed outside the cell but adjacent to a 0.25 mm diameter Pd wire with a thin electroplated coating of Pd, Figures 3a(v) and 4a(ii). A 75 μm Mylar film separated the CR-39 detector and the cathode.

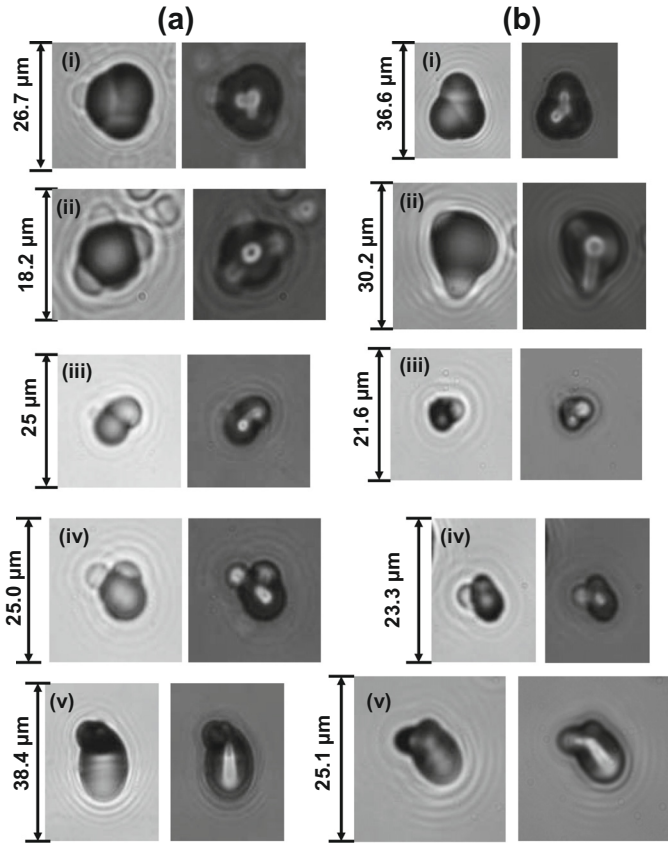

Fig. 3. Symmetric triple tracks observed in CR-39 detectors. (a) Tracks produced in Pd/D co-deposition experiments under the following conditions: (i) Pd electroplated on an Ag wire in a magnetic field. The cathode is in direct contact with the CR-39 detector; (ii) Pd electroplated on an Ag wire in the absence of an external magnetic field. The cathode is in direct contact with the CR-39 detector; (iii) Pd electroplated on an Au wire in a magnetic field. A 60 μm film of polyethylene separates the cathode and the CR-39 detector; (iv) Pd electroplated on an Ag wire in a magnetic field. A 60 μm film of polyethylene separates the cathode and the CR-39 detector; (v) Pd wire with a thin coating of electroplated Pd in a magnetic field. The CR-39 detector is outside the cell. (b) Tracks produced upon exposure to DT generated neutrons. In both (a) and (b), the left-hand image was obtained with the optics focused on the surface of the CR-39 detector while the right-hand image is an overlay of two photomicrographs taken at different focusing depths (surface of the detector and the bottom of the pits).

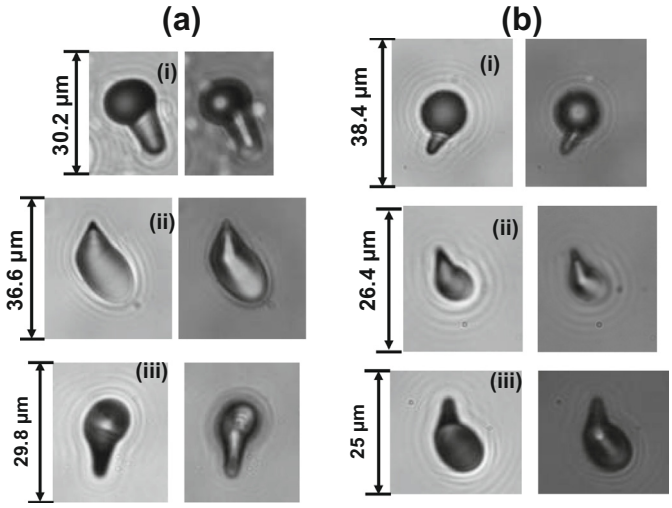

Fig. 4. Asymmetric triple tracks observed in CR-39 detectors. (a) tracks produced in Pd/D co-deposition experiments under the following conditions: (i) Pd electroplated on a Au wire in a magnetic field. A 60 μm film of polyethylene separates the cathode and the CR-39 detector; (ii) Pd wire with a thin coating of electroplated Pd in a magnetic field. The CR-39 detector is outside the cell; (iii) a second experiment in which Pd was electroplated on a Au wire in a magnetic field. A 60 μm film of polyethylene separates the cathode and the CR-39 detector. (b) Tracks produced upon exposure to DT generated neutrons. In both (a) and (b), the left-hand image was obtained with the optics focused on the surface of the CR-39 detector while the right-hand image is an overlay of two photomicrographs taken at different focusing depths (surface of the detector and the bottom of the pits).

The tracks shown in Figure 3 are examples of symmetric triple tracks. Focusing deeper inside the tracks, it can be seen that there are three alpha particles breaking away from a center point. As discussed vide supra, these features are diagnostic of the carbon breakup reaction. Comparing the Pd/D co-deposition results, Figure 3a, with those obtained upon exposure to a DT neutron source, Figure 3b, the triple tracks look very similar. For example, if the track in Figure 3a(i) was rotated downwards, it would look exactly like the DT neutron generated track shown in Figure 3b(i). Likewise, if the DT neutron generated track in Figure 3b(v) were rotated counterclockwise along its major axis and pointed downwards, it would look exactly like the Pd/D generated track shown in Figure 3a(v). The sizes of the triple tracks shown in Figure 3 relative to one another is not relevant as the ^{12}C(n, n$'$)3α carbon breakup reaction can occur anywhere on the surface or inside the CR-39 detector. After etching, triple tracks generated close to the surface of the detector will appear larger than those created deeper inside, as shown in Figure 1. Another complication is that the triple tracks shown in Figure 3 were observed on different CR-39 detectors from different batches. Even within a given batch, variability in the etch rates of the detectors has been observed and this will be reflected in the relative sizes of the tracks. The ^{12}C(n, n$'$)3α carbon breakup reaction is anisotropic. This is illustrated in Figures 3a(iii) and 3b(iii). Both figures show that, as the carbon atom shattered, two alpha particles have been ejected above the plane of the center point. The third alpha particle track is barely visible and indicates that third alpha particle shot below the plane of the center point. Furthermore, the third alpha particle track in Figure 3b(iii) is more visible that the third alpha in Figure 3a(iii). This indicates the carbon break-up reaction that generated the triple track in Figure 3a(iii) occurred more perpendicular to the surface than the reaction that created the triple track shown in Figure 3b(iii). The examples of Pd/D and DT neutron generated tracks shown in

Figure 3 do not have the exact same shape. For the tracks shown in Figures 3a(iv), 3b(iv), 3a(v) and 3b(v), the lobes making up the triple track do not all have the same size. Clearly one lobe is bigger than the other two, which are of similar size. The n + ^{12}C reaction can proceed to the four-body final state through one or more of the following reaction mechanisms [26]:

$$\mathrm{n} + {}^{12}\mathrm{C} \rightarrow \mathrm{n}' + \alpha + {}^{8}\mathrm{Be} \quad (1)$$
$$\hookrightarrow 2\alpha$$

$$\mathrm{n} + {}^{12}\mathrm{C} \rightarrow \alpha + {}^{9}\mathrm{Be} \quad (2a)$$
$$\hookrightarrow \mathrm{n}' + {}^{8}\mathrm{Be}$$
$$\hookrightarrow 2\alpha$$

$$\mathrm{n} + {}^{12}\mathrm{C} \rightarrow \alpha + {}^{9}\mathrm{Be} \quad (2b)$$
$$\hookrightarrow \alpha + {}^{5}\mathrm{He}$$
$$\hookrightarrow \mathrm{n}' + \alpha$$

$$\mathrm{n} + {}^{12}\mathrm{C} \rightarrow {}^{8}\mathrm{Be} + {}^{5}\mathrm{He} \quad (3)$$
$$\hookrightarrow \mathrm{n}' + \alpha$$
$$\hookrightarrow 2\alpha$$

$$\mathrm{n} + {}^{12}\mathrm{C} \rightarrow \mathrm{n}' + \alpha + \alpha + \alpha. \quad (4)$$

Processes (1)−(3) are sequential decays going through different excited states of intermediate systems and process (4) is a simultaneous four-body break-up. The triple track shown in Figure 2b(i) is an example of the four-body break-up event. The observed relative sizes and shapes of the lobes comprising the triple tracks in Figure 3 may be reflective of these different processes. For example, the ^{9}Be recoil has a higher ionization rate and, since that the cone angle decreases with increasing ionization rate, has a smaller cone angle [27].

Examples of asymmetric, apparently two-pronged, tracks for the carbon breakup reaction are shown in Figure 4. Such tracks could be due to the fact that the third prong is below the plane of the detector and is, therefore, not visible. It could also be due to energetics. One of the three alphas particles may not have sufficient energy to make an etchable track and, consequently, cannot be observed [27]. For CR-39, they could also be due to reactions of the type ^{12}C(n, α)^{9}Be or ^{16}O(n, α)^{13}C [28]. The track caused by these reactions typically has one prong with a bigger cone angle than the other which are attributed to the alpha particle and the recoiling residual nucleus, respectively.

3.4 Summary of control experiments

SSNTDs such as CR-39, integrate nuclear tracks passively over their entire lifetime. Consequently, it must be shown that the observed triple tracks resulted from the Pd/D co-deposition process and not from background exposure to ≥9.6 MeV neutrons or to exposure to a DT neutron source. In these experiments, Fukuvi CR-39 is used that had been laser cut into 1 cm by 2 cm rectangular pieces. The detectors come with 60 μm thick polyethylene covers over them that, according to linear energy transfer (LET) curves calculated using the SRIM-2003.26 code of Ziegler and Biersack [29], block 1.8 MeV protons and 7.05 MeV alphas. The polyethylene covers will not block neutrons. The polyethylene covered detectors are stored, in their metallized shipping pouch, in a refrigerator that is in a subterranean room. Prior to use, a corner of the detector is exposed to an ^{241}Am alpha source. This provides an internal calibration for the detector. Blank detectors, not used in Pd/D co-deposition experiments, show solitary tracks. The track density is ∼85 tracks cm^{-2}. No triple tracks were observed in these blank detectors indicating that the triple tracks observed in the Pd/D co-deposition experiments were not the result of DT neutron irradiation of the detectors or to cosmic ray spallation neutrons. Nakamura et al. [30] have measured the energy spectrum of cosmic-ray-induced spallation neutrons and found it consists of three peaks: thermal, 1 MeV evaporation and a cascade peak at 100 MeV. The evaporation peak overlaps the DD fusion 2.45 MeV neutron energy. However, the 12−17 MeV neutron energies, overlapping DT Fusion neutrons with a nominal 14.1 MeV energy, occur an order of magnitude less frequently than either evaporation or cascade neutrons. The total measured background spallation neutron flux was 7.5×10^{-3} n cm^{-2} s^{-1}, with $<10^{-4}$ n cm^{-2} s^{-1} in the DT fusion neutron energy range. This, coupled with the CR-39 relative neutron detection inefficiency, $<10^{-6}$ for triple tracks [20], accounts for the complete absence of triple tracks in the background.

Additional control experiments indicate that the triple tracks observed in the CR-39 detectors used in the Pd/D co-deposition experiments are not due to either chemical or mechanical damage nor are they due to artifacts in the plastic. Some experiments were conducted with a 60 μm thick polyethylene film between the cathode and the detector. This film acts as a chemical/mechanical barrier. In these polyethylene film, Pd/D co-deposition experiments, a significant number of other tracks were observed in addition to the triple tracks. The number of tracks was comparable to what was observed in those experiments conducted with the cathode in direct contact with the detector. The LET curves indicate that these additional tracks could be due to >7.05 MeV alphas, >1.8 MeV protons, and/or neutron recoils. It should be noted that control experiments were conducted by electroplating copper instead of palladium. For both the Pd and Cu electroplating, similar chemical and electrochemical reactions are occurring on the surfaces of the electrodes, i.e. a metal plates out in the presence of evolving deuterium gas at the cathode while oxygen and chlorine gas evolution occurs at the anode. Both Cu and Pd deposits exhibit cauliflower-like morphologies. The only significant difference between the Cu and Pd electroplating experiments is that metallic Pd absorbs deuterium and Cu does not. Because similar chemical and electrochemical reactions are occurring on like morphologies, it is expected that the electrical double layers for the two systems will be comparable. As in the Pd/D co-deposition experiments, the 60 μm thick polyethylene film was placed between the detector and the cathode onto which the copper was plated. Upon etching,

no triple tracks were observed in the Cu electroplating experiments. The number of solitary tracks was comparable to what was observed in blank detectors.

Other control experiments involved electrolysis of either H_2O or D_2O on either Ag wire or Ni screen [14]. No palladium salts were present in these particular experiments. In these experiments, H_2/D_2 gas evolution occurs at the cathode and O_2 gas evolution occurs at the anode. The electrochemical/chemical are the same as are the double layers for both the H_2O/D_2O systems. For both H_2O/D_2O systems, in the absence of palladium salts, the number of tracks in the CR-39 detectors were comparable to that observed in blank detectors. No triple tracks were observed in any of the detectors used in these particular experiments.

In the experimental configuration in which the CR-39 detector was placed outside the cell, a substantial drop in the number of tracks was observed compared to the 60 μm polyethylene spacer experiments described vide supra. Also a 75 μm thick sheet of Mylar separated the cathode from the CR-39 detector. What tracks were observed occurred in clusters. Tracks were observed on both the front and back surfaces of the CR-39. Part of the reason for the decrease in tracks is due to the lengths of the experiments. In these particular experiments, the CR-39 was exposed to the cathode for approximately 24 h. For the 60 μm polyethylene spacer experiments described vide supra, the detector exposure to the cathode was on the order of two weeks and encompassed both the plating and water electrolysis phases of the experiment. Another reason for the observed decrease in tracks in the Pd wire experiment is due to the cathode. The 60 μm polyethylene spacer experiment cathodes consisted of a thick, mossy deposit of Pd that was created using the Pd/D co-deposition process on either an Ag or Au wire. In the "outside the cell" experimental configuration, the cathode is a 0.25 mm diameter Pd wire onto which a thin coating of Pd had been plated out. Consequently, this cathode is primarily bulk Pd. Earlier CR-39 experiments conducted with Pd wire showed that the density of tracks was far less than what was observed for the Pd/D co-deposition experiments and that the distribution of tracks was inhomogeneous [14]. In contrast tracks were homogeneously distributed along the Pd deposit prepared as a result of Pd/D co-deposition. The inhomogeneous distribution of the tracks observed in these earlier Pd wire experiments suggested that some areas of the bulk Pd exhibited greater activity than others. Previous observations [31] have shown that the generation of heat, tritium, and helium does not occur homogeneously throughout the bulk Pd. This indicates that the reactions occur in localized areas within the bulk Pd. Metallurgical aspects of bulk Pd are still not fully understood. The fact that the tracks in the CR-39 detectors used in the "outside the cell" experiments occurred in clusters further confirms that some areas of the Pd wire are more active than others. Furthermore, the triple tracks shown in Figures 3a(v) and 4a(ii) were observed on different CR-39 detectors and were the only triple tracks observed on those detectors.

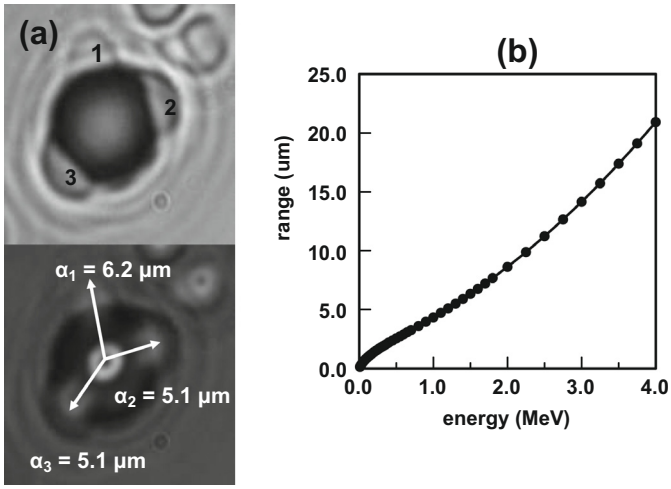

Fig. 5. (a) Photomicrographs of the triple track shown in Figure 2a(ii). The top image was obtained with the optics focused on the surface of the CR-39 detector. The bottom image is an overlay of two photomicrographs taken at different focusing depths (surface of the detector and the bottom of the pits). On the bottom image, the bright circle observed in the track indicates where the neutron impacted the carbon atom. Arrows are drawn to show the directions the alpha particles traveled after the carbon atom shattered. The distances traveled by the alpha particles are indicated. (b) Linear energy transfer (LET) curve for alpha particles in CR-39 calculated using the SRIM-2003.26 code of Ziegler and Biersack [29].

3.5 Calculation of the neutron energy

The threshold energy of the neutron required to shatter a carbon atom to form a triple track is 9.6 MeV [22]. Knowing the threshold energy needed to shatter a carbon atom and the energy of each alpha particle that was created, the energy of the neutron that created the triple track can be calculated using by the following relationship:

$$E_n = E_{th} + E_{\alpha 1} + E_{\alpha 2} + E_{\alpha 3} \quad (5)$$

where E_n and E_{th} are the energy of the neutron causing the triple track and the threshold energy required to shatter a carbon atom, respectively, and $E_{\alpha 1}$, $E_{\alpha 2}$, and $E_{\alpha 3}$ are the energies of the alpha particles formed when the carbon atom shattered. Figure 5a shows a photomicrograph of a triple track that resulted from a Pd/D co-deposition experiment. In the top image of Figure 5a, the lobes attributable to the alpha particles are numbered while the bottom image indicates the direction of movement from the center point as well as the distance traveled by each alpha particle. The uncertainty in the alpha particle distance traveled is ± 0.4 μm. There are two simple methods that can be used to estimate the energies of the alpha particles. One is to use the LET curve for alphas in CR-39, Figure 5b. Knowing the distance traveled by the alpha particle, the LET curve can be used to determine the energy of that alpha particle. For alpha particles 1, 2, and 3 in Figure 5a, the energies of the particles are 1.46 ± 0.09 MeV, 1.21 ± 0.09 MeV, and 1.21 ± 0.09 MeV,

Table 1. Measured and calculated track parameters for the alpha tracks comprising the triple track shown in Figure 5a. Etch time is 6 h and etch rate is 1.25 μm h^{-1}.

	Measured values			Calculated values		
Alpha track	Major axis (μm)	Minor axis (μm)	Energy (MeV)	Incident Angle (°)	Major axis (μm)	Minor axis (μm)
1	7.2 ± 0.4	4.6 ± 0.4	1.3	22.5	7.28	4.60
2	7.6 ± 0.4	5.2 ± 0.4	1.2	25	7.42	5.26
3	7.2 ± 0.4	5.4 ± 0.4	1.15	25	7.21	5.16

respectively. Using equation (5), the resultant neutron energy is estimated to be 13.46 ± 0.16 MeV.

The other method of estimating the neutron energy requires modeling of the alpha particles using the TRACK_TEST program developed by Nikezic and Yu [32,33]. Results of using this method are summarized in Table 1. To use this method, the etch time and etch rate need to be known. These parameters have been measured and are indicated in Table 1. The major and minor axes of the alpha tracks also need to be measured and these are also summarized in Table 1. In the TRACK_ETCH program, there are three forms of the track etch rate function available for use. These three forms exist because the quality of the CR-39 detectors varies between different manufacturers. For the Fukuvi CR-39 detectors used in these experiments, the optimum track rate function was found to be [34]:

$$V_T = V_B \left(e^{(-a_1 x + a_4)} - e^{(-a_2 x + a_3)} + e^{a_3} - e^{a_4} + 1 \right) \quad (6)$$

where V_T and V_B refer to the rates of etching the track and the bulk respectively and x is the residual range of the alpha particle. The values of the coefficients are $a_1 = 0.1$, $a_2 = 1$, $a_3 = 1.27$, and $a_4 = 1$. The results of the track modeling, Table 1, indicates that the three alpha particles have energies of 1.3, 1.2, and 1.15 MeV. The uncertainty in these measurements is estimated to be ± 0.1 MeV. Using equation (5), the resultant neutron energy using this method is estimated to be 13.25 ± 0.17 MeV. The estimated neutron energy calculated using the two methods are, within the uncertainties, in agreement. These calculations assume that the neutron reaction with the detector occurred close to the surface of the detector.

3.6 Discussion of the origins of triple tracks in Pd/D co-deposition experiments

A great deal of research has been done in the area of plasma fusion and the fusion reactions, under plasma conditions, identified. The primary, (7) and (8), and secondary, (9) and (10) plasma fusion reactions are [4]:

$$\mathrm{D} + \mathrm{D} \rightarrow \mathrm{T}\ (1.01\ \mathrm{MeV}) + \mathrm{p}\ (3.02\ \mathrm{MeV}) \quad (7)$$

$$\mathrm{D} + \mathrm{D} \rightarrow \mathrm{n}\ (2.45\ \mathrm{MeV}) + {}^3\mathrm{He}\ (0.82\ \mathrm{MeV}) \quad (8)$$

$$\mathrm{D} + \mathrm{T}\ (\leq 1.01\ \mathrm{MeV}) \rightarrow \alpha\ (6.7\text{–}1.4\ \mathrm{MeV}) + \mathrm{n}\ (11.9\text{–}17.2\ \mathrm{MeV}) \quad (9)$$

$$\mathrm{D} + {}^3\mathrm{He}\ (\leq 0.82\ \mathrm{MeV}) \rightarrow \alpha\ (6.6\text{–}1.7\ \mathrm{MeV}) + \mathrm{p}\ (12.6\text{–}17.5\ \mathrm{MeV}). \quad (10)$$

Researchers have conducted experiments looking for evidence of these reaction products in the Pd/D system. Lipson et al. [8] prepared 8–300 μm thick Au/Pd/PdO heterostructures. These heterostructures were then electrochemically loaded with deuterium. After loading, the samples were removed from the electrolysis cells and nuclear measurements were conducted while deuterium desorbed from the samples. Using CR-39 detectors, 1.0 MeV tritons and 3.0 MeV protons were detected. The flux of proton emissions was estimated to be 0.004 ± 0.001 p/s in a 4π solid angle. Neutron emissions during deuterium desorption of the Au/Pd/PdO:D heterostructures were measured using NE-213 liquid scintillator detectors. The neutron energy was determined to be 2.45 MeV and the flux was 0.019 ± 0.002 n/s in a 4π solid angle. Using the sequential etching method for CR-39 described vide supra, Lipson et al. [21] detected proton recoils inside the detector used in a Pd/D co-deposition experiment conducted on a Ag wire. In this experiment, a 60 μm polyethylene film separated the CR-39 detector from the cathode and the charging protocol was the same as that used in the 60 μm polyethylene film protocols described in these investigations. No proton recoils were detected in the blank CR-39 detectors. The neutron energy was estimated to be in the 2.2–2.5 MeV range and the rate of neutron emission, accounting for the 4π solid angle, was estimated at 1–3 n/s.

Taniguchi et al. [35] used a silicon barrier detector to detect charged particles during electrolysis. They used both Pd foils and Pd layers deposited on stainless steel or Cu foils as the cathodes. The backside of these cathodes was placed on top of the silicon barrier detector. Count rates above background were observed for electrolysis experiments done in D_2O but not for H_2O. The energy spectra obtained for the D_2O showed an increased number of counts between 0.5 and 2 MeV. Taking into account energy losses, they attributed the species giving rise to the increased count rates to 3.03 MeV protons. There have been additional reports of neutron [36–38] and tritium [39–41] emissions in the Pd/D system. However, the detection systems in these experiments were not capable of measuring the energies of the emitted particles.

As discussed vide supra, other tracks, besides the triple tracks, have been observed in CR-39 detectors used in Pd/D co-deposition experiments [13–15]. However, what is observed at the detector is the energy of the particle after its birth and after it has traversed through Pd and water layers to impact the detector. It has been shown that the size and shape of the tracks observed on the

detector are consistent with 1 MeV alpha tracks [42]. Consequently, at their birth, the particles that created these tracks were far more energetic. It is likely that the particles are 1 MeV tritons, 3 MeV protons, and 1−7 MeV alphas. Before Lipson et al. [21] did sequential etching of the CR-39 detector used in the Pd/D co-deposition experiment described vide supra, that detector was analyzed using an automated scanner. The scanned results showed a large number of tracks with major axis between 0 and 3.5 μm. Oda et al. [43] did sequential etching of CR-39 exposed to 10 MeV protons. The track diameters were 1.0 and 2.6 μm after removing 6.5 and 15 μm of plastic, respectively. Therefore, these small tracks are attributed to $\geq$10 MeV protons.

Roussetski [9] conducted experiments using PdO/Pd/PdO and PdO/Pd/Au heterostructures. The experimental protocol was the same as that used by Lipson et al. [8]. The heterostructures were electrochemically loaded with deuterium. Once loaded, the heterostructures were removed from the electrolysis cells and placed in contact with CR-39 detectors. Analysis of the detectors showed the presence of triple tracks. In fact, this was the first report on the observation of triple tracks in CR-39 detectors used in Pd/D experiments. He indicated that "the presence of three α-particle tracks outgoing from a single point allows us to separate these (carbon break-up) reactions from other neutron interactions with CR-39 detectors". From his analysis of the CR-39 detectors used in these experiments, Roussetski concluded that the number of tritons needed to account for the observed triple tracks in the detectors was greater than the yield of tritons from DD reactions. He speculated that there was an unknown nuclear reaction that created the high-energy neutrons and suggested that the process may be the 3D and 4D fusion reactions predicted by Takahashi [44]. In this communication, an alternative explanation is suggested, i.e., the metal lattice creates conditions that favor the DT reaction. If this is the case, tritons will be consumed shortly after birth to create 11.9−17.2 MeV neutrons. This would explain Roussetski's observation that there are more triple tracks than can be accounted for by the number of tritons as only those tritons not consumed in the secondary reaction shown in equation (9) will be registered on the CR-39 detector. There are two conditions which must be met in order for DT reactions to occur – the triton needs to be energetic and it needs to encounter a deuterium atom. Both Lipson et al. [8] and Roussetski [9] have identified tracks due to tritons in their CR-39 detectors used in their PdO/Pd/PdO and PdO/Pd/Au heterostructures experiments. The threshold energy for a triton to create a track in CR-39 is 0.1 MeV [45]. Therefore, the triton that is created inside the Pd lattice is energetic. With regards to the second condition, it has been shown that the deposit formed as a result of Pd/D co-deposition is fully loaded with deuterium, i.e., D/Pd $>$ 1 [46]. LET calculations indicate that a 1 MeV triton will traverse through 4.12 μm of Pd. Given the high density of D inside the Pd lattice, it is highly likely that the energetic triton will encounter a D atom as it races, in any direction, through the lattice. In addition, the cross section of DT fusion is higher than that of DD fusion [47]. Essentially what may be occurring inside the Pd lattice is analogous to what is observed in accelerator experiments involving stationary targets and ion beams such as the neutron generator used to create the tracks shown in Figure 1. The significant difference is that, in the Pd/D system, the triton beam is essentially produced in situ.

The earlier report on triple tracks in CR-39 resulting from Pd/D co-deposition estimated the neutron energies to be between 12.6 to 15.44 MeV [17]. The LET curve method described vide supra was used to estimate these energies. In this investigation, it is shown that the shapes of the observed triple tracks are indistinguishable from DT neutron generated triple tracks and that the energy of the neutron can be estimated using alpha track modeling methods.

In conclusion, experiments have been conducted by a number of different researchers using different methods and/or protocols. Using these methods, charged particles and neutrons, of the appropriate energies, have been detected that are consistent with the primary and secondary fusion reactions shown in equations (7)–(10).

4 Conclusions

Triple tracks have been observed in CR-39 detectors used in Pd/D co-deposition experiments. These triple tracks are indistinguishable from those generated using a DT neutron source. Both symmetric and asymmetric triple tracks have been observed. The most likely source of the neutrons responsible for the triple tracks is DT fusion inside the Pd lattice. This is supported by the observations of charged particles and neutrons consistent with primary and secondary fusion reactions. However, the possibility that these neutrons are created by an unknown nuclear process, as suggested by Roussetski, cannot be ruled out. Although theories are currently under development, the mechanism by which nuclear reactions can occur in Pd is not yet fully understood. However, the Cu electroplating experiments and D_2O electrolysis experiments done on Ag wire and Ni screen, which gave no tracks in the CR-39, indicate that the deuterium needs to be inside a metal lattice in order for these reactions to occur. This is supported by reports of the emission of neutrons [48–50], charged particles [51], and tritium [50] for the Ti/D system. Titanium is another metal that absorbs hydrogen isotopes. Also, the cauliflower-like morphology of electroplated Pd, produces far more energetic particles than bulk Pd indicating that Pd globules with nanoscale dimensions create a favorable environment that enhances these reactions.

This work was funded by the SPAWAR Systems Center Pacific ILIR and S&T Initiatives Programs, the Defense Threat Reduction Agency (DTRA), and JWK Corporation. The authors would also like to thank Dr. G. Phillips, nuclear physicist, retired from the Naval Research Laboratory, US Navy, Radiation Effects Branch, and P. Carbonnelle from *Université*

catholique de Louvain for valuable discussions in interpreting the optical data. It was G. Phillips who first pointed out the existence of triple tracks in our CR-39 photomicrographs. The authors acknowledge the contributions of Dr. S. Szpak, retired from SPAWAR Systems Center Pacific, who pioneered the Pd/D co-deposition process. This manuscript has been co-authored by National Security Technologies, LLC, under Contract No. DE-AC52-06NA25946 with the US Department of Energy. The United States Government retains and the publisher, by accepting the article for publication, acknowledges that the United States Government retains a non-exclusive, paid-up, irrevocable, worldwide license to publish or reproduce the published form of this manuscript, or allow others to do so, for United States Government purposes.

References

1. B.G. Cartwright, E.K. Shirk, P.B. Price, Nucl. Instrum. Meth. **153**, 457 (1978)
2. J.R. Bhakta, G.D. Hardcastle, J.C.H. Miles, Radiat. Meas. **30**, 29 (1999)
3. D. Nikezic, K.N. Yu, Mater. Sci. Eng. R **46**, 51 (2004)
4. J.A. Frenje et al., Rev. Sci. Instrum. **73**, 2597 (2002)
5. F.H. Séguin et al., Rev. Sci. Instrum. **74**, 975 (2003)
6. S.A. Durrani, Radiat. Meas. **43**, S26 (2008)
7. X. Li et al., in *Anomalous Nuclear Effects in Deuterium/Solid Systems*, AIP Conf. Proc. **228** (1991)
8. A.G. Lipson et al., Fus. Technol. **38**, 238 (2000)
9. A.S. Roussetski, in *8th Int. Conf. on Cold Fusion* (Italian Physical Society, Bologna, Italy, 2000)
10. R.A. Oriani, J.C. Fisher, Jpn J. Appl. Phys. **41**, 6180 (2002)
11. A.G. Lipson, A.S. Roussetski, G.H. Miley, C.H. Castano, in *9th Int. Conf. Cold Fusion, Condensed Matter Nuclear Science* (Tsinghua Univ. Press, Beijing, China, 2002)
12. A.G. Lipson, A.S. Roussetski, G.H. Miley, E.I. Saunin, in *10th Int. Conf. Cold Fusion, Cambridge, MA, USA, 2003*, p. 539
13. S. Szpak, P.A. Mosier-Boss, F.E. Gordon, Naturwissenschaften **94**, 515 (2007)
14. P.A. Mosier-Boss, S. Szpak, F.E. Gordon, L.P.G. Forsley, Eur. Phys. J. Appl. Phys. **40**, 293 (2007)
15. P.A. Mosier-Boss, S. Szpak, F.E. Gordon, L.P.G. Forsley, Eur. Phys. J. Appl. Phys. **46**, 30901 (2009)
16. P.A. Mosier-Boss, S. Szpak, F.E. Gordon, L.P.G. Forsley, in *Low-Energy Nuclear Reactions Sourcebook*, edited by J. Marwan, S.B. Krivit (American Chemical Society, 2008)
17. P.A. Mosier-Boss, S. Szpak, F.E. Gordon, L.P.G. Forsley, Naturwissenschaften **96**, 135 (2009)
18. G.F. Knoll, *Radiation Detection and Measurement* (John Wiley & Sons, 1979)
19. S.E. Jones, D.E. Jones, D.S. Shelton, S.F. Taylor, Trans. Fus. Technol. **8**, 143 (1994)
20. G.W. Phillips et al., Radiat. Prot. Dosim. **120**, 1 (2006)
21. A. Lipson et al., in *8th Int. Workshop on Anomalies in Hydrogen/Deuterium Loaded Metals, Catania, Sicily, Italy, 2007*, p. 182
22. S.A.R. Al-Najjar, A. Abdel-Naby, S.A. Durrani, Nucl. Tracks **12**, 611 (1986)
23. A.M. Abdel-Moneim, A. Abdel-Naby, Radiat. Meas. **37**, 15 (2003)
24. J.K. Pálfalvi, J. Szab, Y. Akatov, L. Saj-Bohus, I. Eördögh, Radiat. Meas. **40**, 428 (2005)
25. L. Saj-Bohus, J.K. Pálfalvi, Y. Akatov, O. Arevalo, E.D. Greaves, P. Németh, D. Palacios, J. Szab, I. Eördögh, Radiat. Meas. **40**, 442 (2005)
26. B. Antolkoviæ, Z. Dolenec, Nucl. Phys. A **237**, 235 (1975)
27. A. Aframian, J. Phys. G: Nucl. Phys. **9**, 985 (1983)
28. M. Balcázar-García, S.A. Durrani, Nucl. Instrum. Meth. **173**, 131 (1980)
29. J.F. Ziegler, J.P. Biersack, *The Stopping and Range of Ions in Solids* (Pergamon, New York, 1985)
30. T. Nakamura et al., J. Nucl. Sci. Technol. **42**, 843 (2005)
31. E. Storms, in *6th Int. Conf. Cold Fusion, Progress in New Hydrogen Technology* (Tokyo Institute of Technology, Tokyo, Japan, 1996)
32. D. Nikezic, K.N. Yu, Radiat. Meas. **37**, 39 (2003)
33. D. Nikezic, K.N. Yu, Comput. Phys. Commun. **174**, 160 (2006)
34. C. Brun et al., Radiat. Meas. **31**, 89 (1999)
35. R. Taniguchi, T. Yamamoto, S. Irie, Jpn J. Appl. Phys. **28**, L2021 (1989)
36. A. Takahashi, T. Takeuchi, T. Iida, M. Watanabe, J. Nucl. Sci. Technol. **27**, 663 (1990)
37. T. Mizuno et al., Jpn J. Appl. Phys. **40**, L989 (2001)
38. A. Shyam, R.K. Rout, IEEE Trans. Plasma Sci. **27**, 1210 (1999)
39. N.J.C. Packham, K.L. Wolfe, R.C. Kainthla, J.O'M. Bockris, J. Electroanal. Chem. **270**, 451 (1989)
40. C.-C. Chien, D. Hodko, Z. Minevski, J.O'M. Bockris, J. Electroanal. Chem. **338**, 189 (1992)
41. S. Szpak, P.A. Mosier-Boss, R.D. Boss, J.J. Smith, Fus. Technol. **34**, 38 (1998)
42. P.A. Mosier-Boss, L.P.G. Forsley, F.E. Gordon, J. Condens. Matter Nucl. Sci. **3** (2010) (in press)
43. K. Oda, M. Ito, H. Miyake, M. Michijima, Nucl. Instrum. Meth. Phys. Res. B **35**, 50 (1988)
44. A. Takahashi, Fus. Technol. **26**, 451 (1994)
45. R. Bedogni, Doctoral thesis Universitat Autònoma de Barcelona, 2006
46. S. Szpak, P.A. Mosier-Boss, J.J. Smith, J. Electroanal. Chem. **379**, 121 (1994)
47. J.D. Lawsen, Proc. Phys. Soc. Lond. B **70**, 6 (1957)
48. A. De Ninno, A. Frattolillo, G. Lollobattista, L. Martinis, M. Martone, L. Mori, S. Podda, F. Scaramuzzi, Nuovo Cimento Soc. Ital. Fis. A **101**, 9 (1989)
49. A. De Ninno, A. Frattolillo, G. Lollobattista, L. Martinis, M. Martone, L. Mori, S. Podda, F. Scaramuzzi, Europhys. Lett. **9**, 221 (1989)
50. R.K. Rout, M. Srinivasen, A. Shyam, V. Chitra, Fus. Technol. **19**, 391 (1991)
51. A.S. Roussetski, A.G. Lipson, V.P. Andreanov, in *10th Int. Conf. Cold Fusion, Cambridge, MA, USA, 2003*, p. 559